

Optical Response of Individual Au-Ag@SiO₂ Hetero-Dimers

Anna Lombardi¹, Marcin P. Grzelczak², Aurélien Crut^{1*}, Paolo Maioli¹, Isabel Pastoriza-Santos², Luis M. Liz-Marzán^{2,3,4}, Natalia Del Fatti¹ and Fabrice Vallée¹

¹ *FemtoNanoOptics group, Institut Lumière Matière UMR5306, Université Lyon 1-CNRS, 69622 Villeurbanne, France*

² *Departamento de Química Física, Universidade de Vigo, 36310 Vigo, Spain*

³ *Bionanoplasmonics Laboratory, CIC biomaGUNE, Paseo de Miramón 182, 20009 Donostia-San Sebastián, Spain*

⁴ *Ikerbasque, Basque Foundation for Science, 48011 Bilbao, Spain*

**Corresponding author: aurelien.crut@univ-lyon1.fr*

Content :

- **Text:** Modeling using a dipolar-quasistatic approach.
- **Figure S1:** Dependence of hetero-dimer extinction on Au-Ag separation.
- **Figure S2:** Elliptical nanoparticles: effect of orientation.
- **Figure S3:** Hetero-dimers with complex morphologies.
- **Figure S4:** Absorption and scattering cross-sections computed for the hetero-dimer of Figure 3a.
- **Figure S5:** Spatial distribution of the total electric field in and around isolated Ag@SiO₂ and Au nanoparticles.
- **Figure S6:** Quasistatic computations performed for incident light polarization orthogonal to the dimer axis.

Interaction of the Ag and Au particles assembled in a hetero-dimer can be qualitatively interpreted using a dipolar-quasistatic approach. In this approximated framework, the spatial variation of the incident electromagnetic wave within the silver-gold heterodimers is neglected, and the response of each nanoparticle in the dimer to the electromagnetic field is modeled as that of an induced dipole at the center of the particle. The associated dipole moments $\mathbf{p}_{Au,Ag}$ are obtained from their dipolar polarizabilities $\alpha_{Au,Ag}$ and the local field $\mathbf{E}_{Au,Ag}^{loc}$ at the particle center. For an isotropic particle, $\mathbf{p}_{Au,Ag} = \alpha_{Au,Ag} \epsilon_0 \epsilon_m \mathbf{E}_{Au,Ag}^{loc}$, where ϵ_m is the dielectric constant of the surrounding medium (this is assumed to be homogeneous, neglecting the anisotropy due to the presence of the substrate). The local electric field acting on a particle is the sum of the external field \mathbf{E}^0 due to the incident light wave and that created by the dipole induced in the other particle. For \mathbf{E}^0 parallel or orthogonal to the dimer axis, one thus gets:

$$\begin{cases} E_{//,Ag}^{loc} = E_{//}^0 + \frac{p_{Au}}{2\pi\epsilon_0\epsilon_m l^3} \\ E_{//,Au}^{loc} = E_{//}^0 + \frac{p_{Ag}}{2\pi\epsilon_0\epsilon_m l^3} \end{cases} \quad \begin{cases} E_{\perp,Ag}^{loc} = E_{\perp}^0 - \frac{p_{Au}}{4\pi\epsilon_0\epsilon_m l^3} \\ E_{\perp,Au}^{loc} = E_{\perp}^0 - \frac{p_{Ag}}{4\pi\epsilon_0\epsilon_m l^3} \end{cases}$$

where l is the center to center interparticle distance.

Resolution of the above system provides the polarization dependent effective polarizabilities $\alpha_{Au,Ag}^{eff}$ of the nano-objects composing the dimer (defined as $\mathbf{p}_{Au,Ag} = \alpha_{Au,Ag}^{eff} \epsilon_0 \epsilon_m \mathbf{E}^0$). The total polarizability of the dimer is thus given by $\alpha = \alpha_{Ag}^{eff} + \alpha_{Au}^{eff}$, which for parallel and perpendicular light polarization reads:

$$\left\{ \begin{array}{l} \alpha_{//,Ag}^{eff} = \alpha_{Ag} \frac{1 + \frac{\alpha_{Au}}{2\pi l^3}}{1 - \frac{\alpha_{Ag} \alpha_{Au}}{(2\pi l^3)^2}} \\ \alpha_{//,Au}^{eff} = \alpha_{Au} \frac{1 + \frac{\alpha_{Ag}}{2\pi l^3}}{1 - \frac{\alpha_{Ag} \alpha_{Au}}{(2\pi l^3)^2}} \\ \alpha_{//} = \frac{\alpha_{Ag} + \alpha_{Au} + \frac{\alpha_{Ag} \alpha_{Au}}{\pi l^3}}{1 - \frac{\alpha_{Ag} \alpha_{Au}}{(2\pi l^3)^2}} \end{array} \right. \quad \left\{ \begin{array}{l} \alpha_{\perp,Ag}^{eff} = \alpha_{Ag} \frac{1 - \frac{\alpha_{Au}}{4\pi l^3}}{1 - \frac{\alpha_{Ag} \alpha_{Au}}{(4\pi l^3)^2}} \\ \alpha_{\perp,Au}^{eff} = \alpha_{Au} \frac{1 - \frac{\alpha_{Ag}}{4\pi l^3}}{1 - \frac{\alpha_{Ag} \alpha_{Au}}{(4\pi l^3)^2}} \\ \alpha_{\perp} = \frac{\alpha_{Ag} + \alpha_{Au} - \frac{\alpha_{Ag} \alpha_{Au}}{2\pi l^3}}{1 - \frac{\alpha_{Ag} \alpha_{Au}}{(4\pi l^3)^2}} \end{array} \right.$$

The absorption and scattering cross-sections of the dimer are then deduced from its polarizability using $\sigma_{abs}(\lambda) = 2\pi\sqrt{\varepsilon_m}/\lambda \text{Im}[\alpha(\lambda)]$ and $\sigma_{scat}(\lambda) = (8\pi^3\varepsilon_m^2/3\lambda^4) |\alpha(\lambda)|^2$ and identifying $\alpha_{Au,Ag}$ with the polarizability of an isolated sphere of radius R : $\alpha = 4\pi R^3 \frac{\varepsilon - \varepsilon_m}{\varepsilon + 2\varepsilon_m}$. The measured gold or silver dielectric functions ε are used, and include the effects of both intra- and interband electronic transitions. The computed polarizabilities and cross-sections are plotted in Figure 6 of the main text (parallel polarization) and Figure S6 (orthogonal polarization).

When the distance l separating the dimer components is large ($\alpha_{Ag}, \alpha_{Au} \ll l^3$), first-order development of the polarizabilities then yields:

$$\left\{ \begin{array}{l} \alpha_{//,Ag}^{eff} = \alpha_{Ag} + \frac{\alpha_{Ag} \alpha_{Au}}{2\pi l^3} \\ \alpha_{//,Au}^{eff} = \alpha_{Au} + \frac{\alpha_{Ag} \alpha_{Au}}{2\pi l^3} \\ \alpha_{//} = \alpha_{Ag} + \alpha_{Au} + \frac{\alpha_{Ag} \alpha_{Au}}{\pi l^3} \end{array} \right. \quad \left\{ \begin{array}{l} \alpha_{\perp,Ag}^{eff} = \alpha_{Ag} - \frac{\alpha_{Ag} \alpha_{Au}}{4\pi l^3} \\ \alpha_{\perp,Au}^{eff} = \alpha_{Au} - \frac{\alpha_{Ag} \alpha_{Au}}{4\pi l^3} \\ \alpha_{\perp} = \alpha_{Ag} + \alpha_{Au} - \frac{\alpha_{Ag} \alpha_{Au}}{2\pi l^3} \end{array} \right.$$

Electromagnetic coupling reflects in the polarizability *via* a term proportional to $\alpha_{Ag}\alpha_{Au}/l^3$ and identical for the gold and silver components. As expected from the structure of the electric field of a dipole, the coupling term has opposite signs for parallel and orthogonal polarizations, with a 2-fold larger amplitude in the former case.

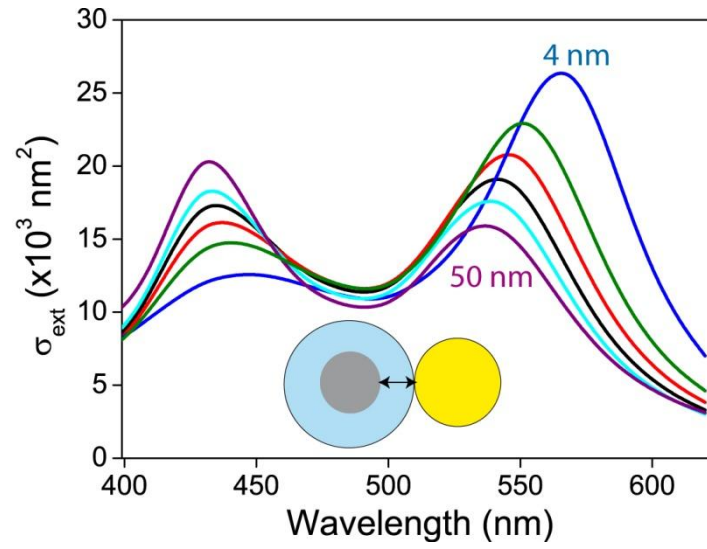


Figure S1. Computed extinction cross-section spectra of hetero-dimers for different silica shell thickness: 4 nm (blue line), 7 nm (green), 10 nm (red), 14 nm (black, same as in Fig. 3c), 20 nm (cyan) and 50 nm (purple). The same particle sizes (R_{Au} , R_{Ag}) and refractive index n_m as in Figure 3c are used.

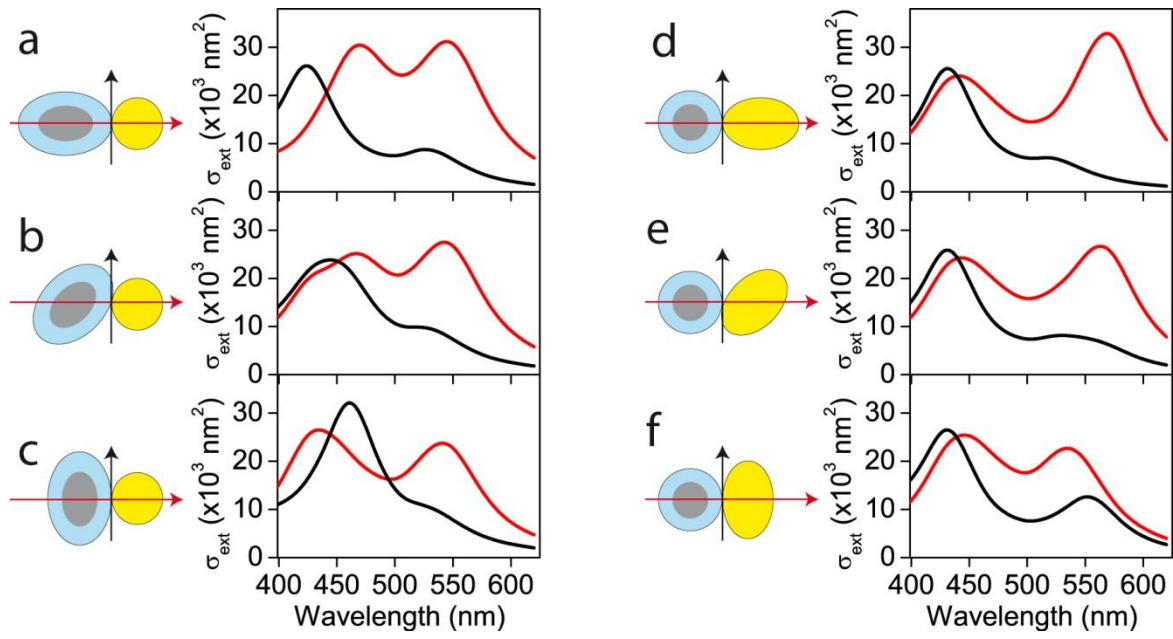


Figure S2. Computed extinction spectra of a hetero-dimer formed by a spherical Au particle and an elliptical Ag@SiO₂ particle for a main Ag ellipsoid axis forming an angle of a) 0°, b) 45° and c) 90° relative to the dimer axis (the same sizes and n_m value as in Figure 4a-c are used). d-f) show the same data for a hetero-dimer formed by a spherical Ag@SiO₂ particle and an elliptical Au particle (same sizes and n_m value as in Figure 4d-f). The red and black lines were computed for light polarized along and perpendicular to the dimer axis, respectively (see schematic drawings).

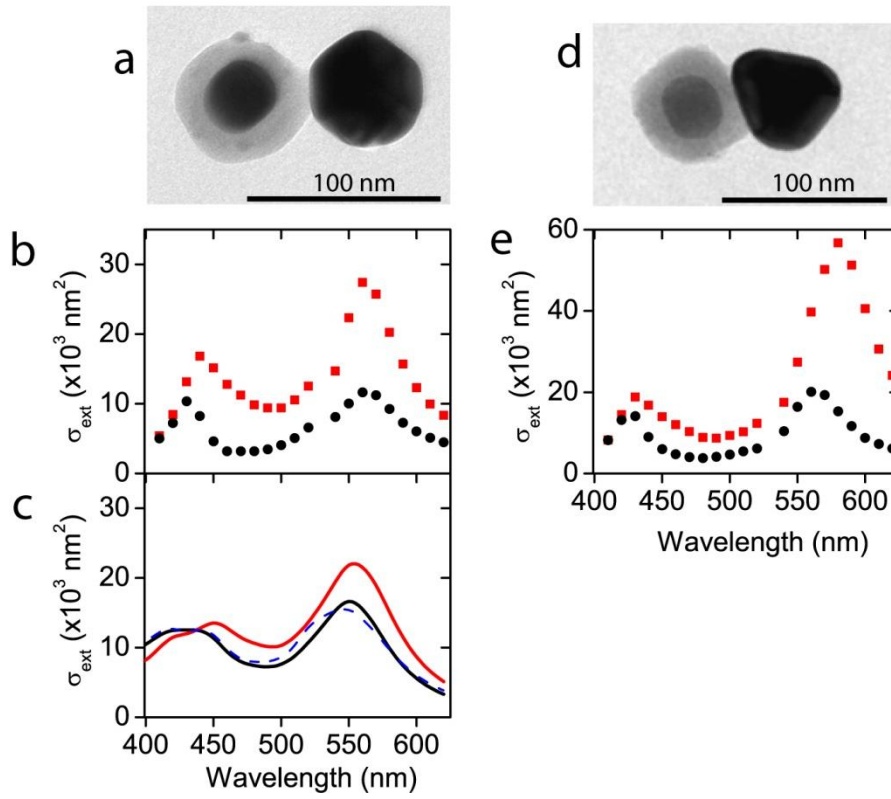


Figure S3. Measured TEM morphology and extinction spectra of a hetero-dimer with one constituting nanoparticle elongated in a direction non orthogonal to the dimer axis (a-b), and for a hetero-dimer with a triangular shape gold component (d-e). The first hetero-dimer is modeled by an almost spherical Au nanoparticle of radius $R_{\text{Au}} = 29.5 \text{ nm}$, and a prolate ellipsoidal Ag@SiO₂ particle (long and short axis of 37 nm and 32 nm, respectively) with a main axis oriented at 45° to the dimer axis. The red and black lines in c) are computed for light polarized parallel and perpendicular to the dimer axis and the dashed blue line is the sum of the computed extinction cross-sections of isolated Au and Ag@SiO₂ with same sizes (identical for the two orthogonal light polarizations). A mean refractive index of the environment above the substrate $n_m = 1.45$ was used in FEM simulations.

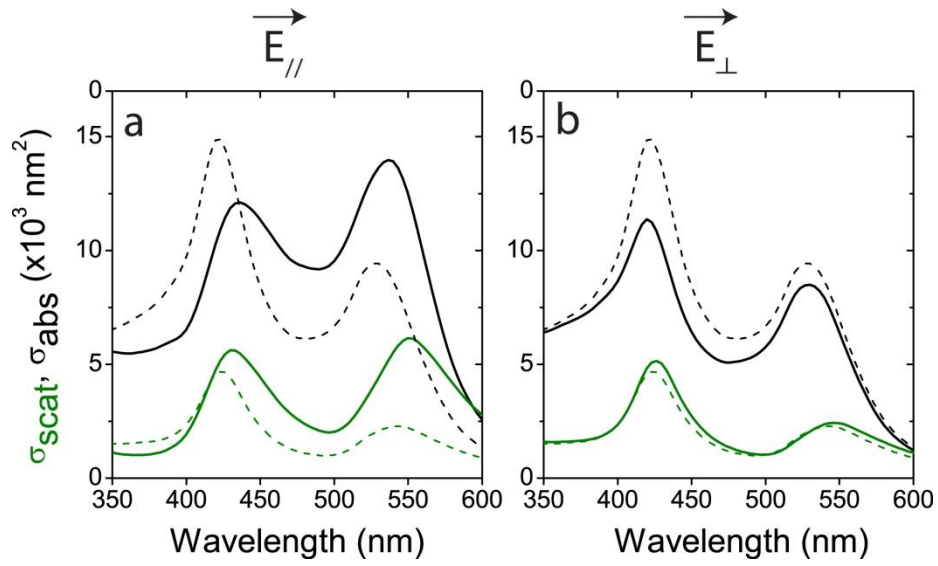


Figure S4. Absorption and scattering cross-sections (plain black and green lines, respectively) computed for the hetero-dimer of Figure 3a, with $R_{\text{Au}} = 29 \text{ nm}$, $R_{\text{Ag}} = 19 \text{ nm}$ and $R_t = 33 \text{ nm}$. The mean refractive index of the environment above the substrate is $n_m = 1.3$. The incident light is polarized in a) parallel ($E_{//}$) and in b) orthogonal (E_{\perp}) to the dimer axis. The dashed black and green lines are the sum of the absorption and scattering cross-sections of isolated Ag@SiO₂ and Au nano-spheres.

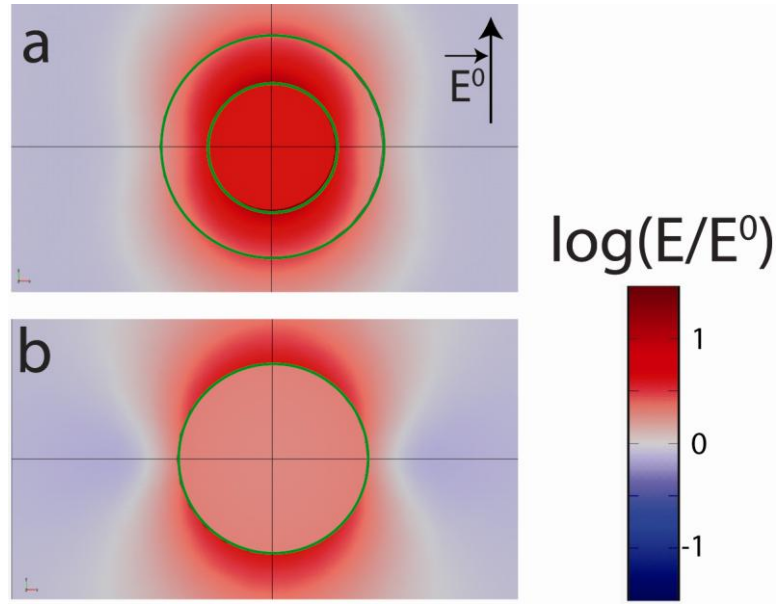


Figure S5. Spatial distribution of the total electric field in and around isolated a) Ag@SiO₂ and b) Au nanoparticles (same sizes and n_m value as in Figure 5 of the main text), computed using FEM. The field was computed at σ_{ext} resonance wavelengths: a) 420 nm for Ag@SiO₂, b) 530 nm for Au. The incident light polarization used in these calculations is shown in a). The electric field amplitude is normalized to that of the incident wave (E^0) and shown on the same color-coded logarithmic scale as in Figure 5.

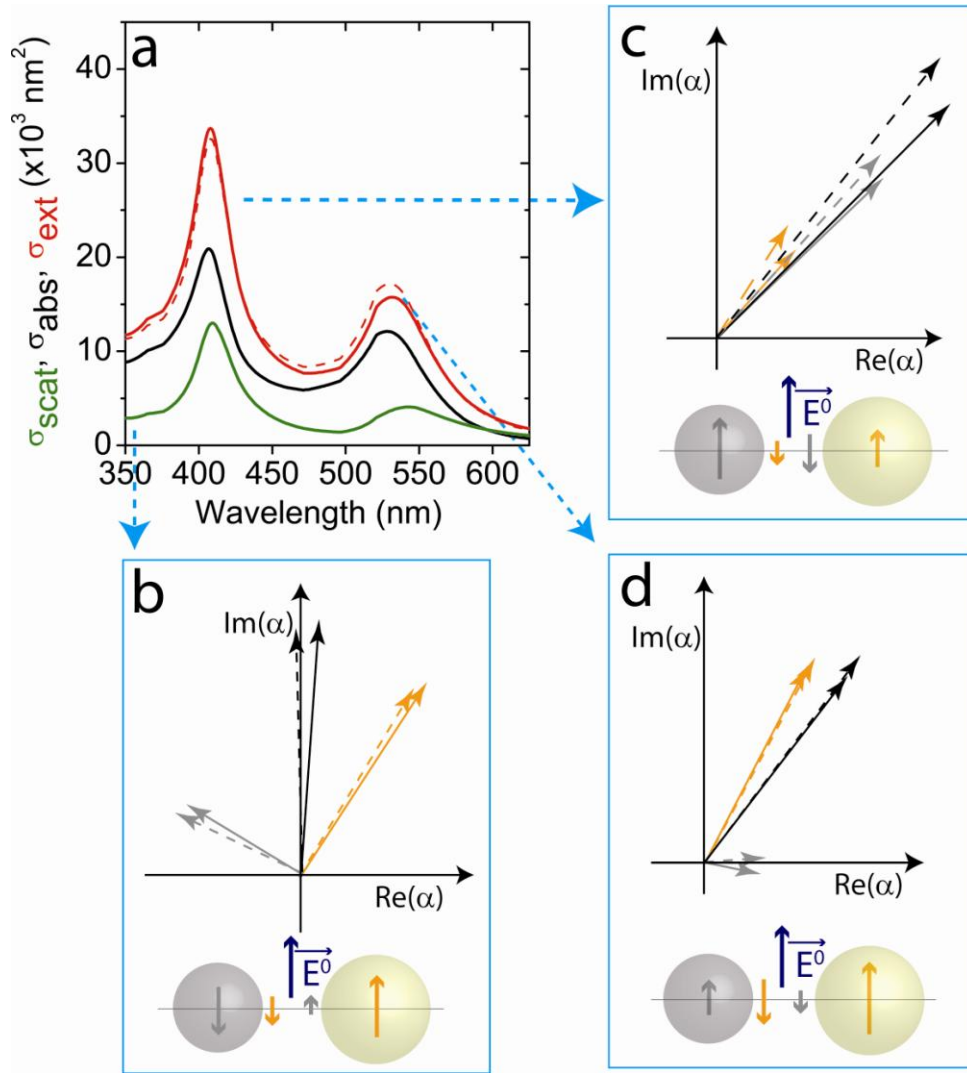


Figure S6: Quasistatic computations performed for incident light polarization orthogonal to the dimer axis. a) Extinction (plain red line), absorption (plain black line) and scattering (plain green line) cross-sections computed for an environment with a uniform 1.45 refractive index. Extinction (dashed red line) cross-section computed by summation of the cross-sections of isolated gold and silver nanoparticles is also shown. b-d) Complex polarizabilities computed at 360 nm (b), 420 nm (c) and 530 nm (d) for the whole dimer (plain black arrows) and its silver (plain grey arrows) and gold (plain orange arrows) components. Polarizabilities in the absence of interaction are shown as dashed lines for comparison.